Title

Measuring Spatiotemporal cAMP Dynamics Within an Endogenous Signaling Compartment Using FluoSTEP-ICUE.

Authors

Hardy, Julia
Mehta, Sohum
Zhang, Jin

Publication Date

2022

DOI

10.1007/978-1-0716-2245-2_22

Peer reviewed

HHS Public Access

Author manuscript

Methods Mol Biol. Author manuscript; available in PMC 2023 March 08.

Published in final edited form as:

Methods Mol Biol. 2022 ; 2483: 351–366. doi:10.1007/978-1-0716-2245-2_22.

Measuring spatiotemporal cAMP dynamics within an endogenous signaling compartment using FluoSTEP-ICUE

Julia C. Hardy[1], **Sohum Mehta**[2], **Jin Zhang**[1,2,3,†]

[1]Department of Bioengineering, University of California San Diego, La Jolla, CA 92093, USA

[2]Department of Pharmacology, University of California San Diego, La Jolla, CA 92093, USA

[3]Department of Chemistry and Biochemistry, University of California San Diego, La Jolla, CA 92093, USA

Abstract

cAMP is a ubiquitous second messenger involved in the regulation of diverse cellular processes. Spatiotemporal regulation of cAMP through compartmentalization within various subcellular microdomains is essential to ensure specific signaling. In the following protocol, we describe a method for directly visualizing signaling dynamics within cAMP microdomain using Fluorescent Sensors Targeted to Endogenous Proteins (FluoSTEPs). Instead of overexpressing a biosensor-tagged protein of interest to target a microdomain, FluoSTEP Indicator of cAMP using Epac (FluoSTEP-ICUE) utilizes spontaneously complementing split GFP and CRISPR-Cas9 genome editing to localize a FRET-based cAMP biosensor to an endogenously expressed protein of interest. Utilizing this approach, FluoSTEP-ICUE can be used to measure cAMP levels within endogenous signaling compartments, thus providing a powerful tool for studying the spatiotemporal regulation of cAMP signaling.

Keywords

Biosensor; FRET; Live-cell Imaging; Compartmentation; Microdomain

1. Introduction

1.1 cAMP/PKA Signaling

3’,5’ -cyclic adenosine monophosphate (cAMP) is a ubiquitous second messenger and a central regulator of cellular functions. cAMP production is typically initiated when an agonist binds to a transmembrane G-protein coupled receptor (GPCR), activating adenylyl cyclases (ACs) to catalyze the production of cAMP from ATP. cAMP signaling proceeds through multiple effector proteins, such as cAMP-dependent kinase (PKA), exchange protein activated by cAMP (Epac), and cAMP-gated channel (CNGC), and is terminated when cAMP is digested by cAMP-degrading phosphodiesterases (PDEs). Through these various effectors, cAMP signaling controls numerous biological processes, including cell

†Correspondence to Jin Zhang: jzhang32@ucsd.edu.

growth, metabolism, and survival [1–11]. Compartmentalization of cAMP elevations within discrete subcellular microdomains is essential for cells to achieve spatiotemporal regulation and ensure specificity in cAMP signaling [12,13]. These cAMP signaling microdomains are frequently implicated in regulating key protein targets of cAMP and its effectors, yet directly investigating the spatiotemporal dynamics of cAMP with respect to specific microdomains can prove challenging.

1.2 FRET-based cAMP Reporters

The spatiotemporal dynamics of cAMP in living cells were first visualized over 30 years ago using a fluorescence resonance energy transfer (FRET)-based biosensor composed of fluorescent dye-conjugated PKA subunits, which dissociate upon cAMP binding, leading to a FRET decrease [14]. While this originally required labeling purified PKA subunits in vitro and then injecting them into living cells, replacing the fluorescent dyes with FRET-compatible FPs later enabled the entire sensor to be genetically encoded and produced directly within cells [15]. A wide variety of genetically encoded FRET-based cAMP indicators have since been developed, greatly enhancing our ability to measure cAMP signaling dynamics in living cells [16–18]. These sensors utilize elements from different cAMP-binding proteins, such as PKA [14,15,19–21], Epac [19,22–29], and CNGC [30], as molecular switches that change conformation upon cAMP binding to modulate FRET between a pair of attached fluorescent proteins. For example, our Indicator of cAMP using Epac (ICUE) probe contains residues 149–881 of Epac1 sandwiched between cyan (CFP) and yellow fluorescent protein (YFP) [23,24,31]. Binding of cAMP to ICUE causes the Epac1(149–881) fragment to adopt a more open conformation, leading to a decrease in FRET [23,24,31].

FRET involves the non-radiative transfer of excited-state energy from a donor (e.g., fluorescent protein) to a compatible acceptor. When FRET occurs, the intensity of donor (e.g., CFP) emission will decrease, and the intensity of acceptor (e.g., YFP) fluorescence emission will increase. In practice, FRET changes are therefore often reported as changes in the acceptor-to-donor (or donor-to-acceptor) emission ratio, although other measurements of FRET efficiency can also be used [32]. The efficiency of energy transfer strongly depends on both close physical proximity (e.g., <10 nm) and correct orientation between the donor and acceptor, which is what renders FRET so highly sensitive to protein conformational changes and allows FRET efficiency to vary with the state of a molecular switch. Energy transfer also depends on the spectral properties of the donor and acceptor. Good FRET pairs, such as CFP and YFP, are characterized by significant overlap of the donor emission spectrum with the acceptor excitation spectrum and minimal overlap between the donor and acceptor excitation spectra.

1.3 Visualizing Local cAMP Signaling Dynamics

cAMP sensors such as ICUE are frequently used to study cAMP dynamics at various subcellular compartments, such as the plasma membrane and mitochondria [23,25,33–36]. This is achieved using endogenously derived sequence motifs that serve as localization signals, which can be appended to the N- or C-terminus of the cAMP biosensor at the DNA level, resulting in targeted expression of the biosensor at the corresponding location.

Even more discrete targeting can be performed by similarly fusing the biosensor sequence to the gene sequence of a protein of interest (POI) that localizes to a cAMP microdomain and overexpressing the resulting fusion protein[33,37,38]. However, overexpressing a POI-tethered cAMP biosensor can perturb the local signaling environment, such as the formation of protein complexes, potentially interfering with the spatiotemporal dynamics of cAMP signaling. If POI expression can instead be maintained at endogenous levels while allowing efficient tagging with a cAMP sensor, local cAMP dynamics can be accurately measured without disrupting the native signaling environment.

To address these concerns, we recently established a new class of biosensors called Fluorescent Sensors Targeted to Endogenous Proteins (FluoSTEPs) (Figure 1) [31] [Tenner et al, 2021, in press] that combines a self-complementing split-superfolder GFP (sfGFP) [39,40] with genome editing to reconstitute a FRET-based biosensor at an endogenously expressed POI. In split-sfGFP [39], the GFP β-barrel is divided into two fragments, strands 1–10 (GFP_{1-10}) plus the 11^{th} strand (GFP_{11}), which can spontaneously and efficiently self-complement. The small size of GFP_{11} (16 amino acids) allows it to be used for efficient tagging of endogenously expressed POIs via CRISPR-Cas9, followed by expression of $GFP_{1–10}$ to reconstitute a fluorescent tag at the POI [40,41]. Similarly, FluoSTEPs utilize $GFP_{1–10}$ as an incomplete FRET donor that can spontaneously reconstitute with a GFP_{11}-tagged POI to achieve biosensor targeting. For example, FluoSTEP-ICUE replaces the YFP acceptor and CFP donor in ICUE3 [23] with mRuby2 and $GFP_{1–10}$, respectively [Tenner et al, 2021, in press] (Figure 1). Self-complementation between the $GFP_{1–10}$ fragment within FluoSTEP-ICUE and an endogenously expressed GFP_{11}-tagged POI will reconstitutes the intact biosensor at the POI. To date, we have successfully used FluoSTEP-ICUE to monitor local cAMP dynamics associated with endogenously expressed PKA RIα during RIα phase separation [31], as well as endogenously expressed clathrin [Tenner et al, 2021, in press].

Below, we provide a detailed protocol for using FluoSTEP-ICUE to study live-cell endogenous cAMP dynamics at a GFP_{11}-tagged POI. This includes detailed procedures for maintaining HEK293T/FT cells, generation of cell lines expressing a GFP_{11}-tagged POI via CRISPR-Cas9, transfection of FluoSTEP-ICUE, preparation of cells for imaging experiments, imaging of FluoSTEP-ICUE FRET responses in live cells, and analysis of the acquired imaging data to calculate the FluoSTEP-ICUE emission ratio and quantify changes in cAMP levels.

2. Materials

2.1 Stock Solutions

1. D-PBS (Dulbecco’s phosphate-buffered saline; without Mg^{2+} and Ca^{2+}, 1X, Gibco)
2. HBSS* (Hank’s Balanced Salt Solution for Imaging): 1X HBSS (Gibco) supplemented with 20 mM HEPES (Invitrogen) and 2 g/L D-glucose (Sigma). Adjust pH to 7.4 and sterilize with 0.22 μm filter. Store at 4 °C.

3. FACS (Fluorescence Activated Cell Sorting) Buffer (1X stock, made in house, pH to 7, sterilize with 0.22 μm filter, store at 4 °C): 0.05% w/v BSA, 25 mM HEPES, 1 mM EDTA, 2.5 μg/mL DNase I, 0.1 μg/mL DAPI, 1X D-PBS
4. Trypsin-EDTA: solution of Trypsin (0.05%) and EDTA (ethylenediamine tetra-acetic acid; 0.53 mM) (store at −20 °C). (Invitrogen) (*see* Note 1)
5. Puro (Puromycin; 2 mg/mL in ddH_2O, store at −20 °C) (Sigma-Aldrich)
6. Optional drugs for cAMP stimulation or PDE inhibition:
   a. Fsk (Forskolin; 50 mM in DMSO, store at −20 °C) (Calbiochem)
   b. Iso (Isoproterenol; 10 mM in DMSO, store at −20 °C) (Sigma-Aldrich)
   c. IBMX (3-isobutyl-1-methylxanthine; 100 mM in DMSO, store at −20 °C) (Sigma-Aldrich)

2.2 Cell Culture and Transfection

1. Cell lines: HEK 293T (Human Embryonic Kidney – SV40 T Antigen) and HEK 293FT (Human Embryonic Kidney – SV40 large T Antigen) (*see* Note 1)
2. DMEM (Dulbecco Modified Eagle Medium; Gibco) (*see* Note 1)
   a. HEK 293T/293FT media: DMEM containing 4.5 g/L glucose, L-Glutamine, 110 mg/L Sodium Pyruvate with phenol red, and supplemented with 10% (v/v) fetal bovine serum (FBS, Sigma) and 1% (v/v) penicillin-streptomycin (Pen-Strep, Sigma-Aldrich)
   b. Transfection media (high-glucose, serum-free): DMEM containing 4.5 g/L glucose, L-Glutamine, 110 mg/L Sodium Pyruvate with phenol red, and supplemented with 1% (v/v) Pen-Strep
   c. FACS media: DMEM containing 4.5 g/L glucose, L-Glutamine, 110 mg/L Sodium Pyruvate with phenol red, and supplemented with 20% (v/v) FBS and 1% (v/v) Pen-Strep (*see* Note 2)
3. PolyJet (SignaGen Laboratories) (*see* Note 1)
4. FluoSTEP-ICUE plasmid
5. px459 plasmid (Golden Gate)
6. 60-mm and 10-cm cell culture treated dishes (Corning)
7. 35-mm glass-bottom imaging dishes (14-mm glass bottom; Cellvis)
8. 24- and 96-well plates (Eppendorf)
9. 1.5 mL microcentrifuge tubes (Falcon)

2.3 Epifluorescence Microscope

1. All of the experiments described below are performed on a Zeiss Axiovert 200M microscope (Carl Zeiss) with a 40x/1.3 NA oil-immersion objective and an ORCA-Flash4.0LT digital CMOS camera (Hamamatsu) in a dark room.
2. Xenon lamp: XBO 75 W (Zeiss)
3. Neutral density filters 0.6 and 0.3 (Chroma Technology)
4. Filter set for individual channels (Chroma Technology):

   GFP direct: 480DF30 excitation filter, 505DRLP dichroic mirror, 535DF45 emission filter

   RFP direct: 568DF55 excitation filter, 600DRLP dichroic mirror, 653DF95 emission filter

   G-R FRET: 480DF30 excitation filter, 505DRLP dichroic mirror, 653DF95 emission filter

   Lambda 10–2 filter-changer (Sutter Instruments) to alternate filters
5. Immersion oil “Immersol” 518F fluorescence free (Ziess)
6. METAFLUOR 7.7 software (Molecular Devices) (*see* Note 3)

2.4 Image Analysis

1. METAFLUOR 7.7 software to analyze images (*see* Note 3)
2. Microsoft Excel and/or GraphPad Prism software (or equivalent) for graphing imaging analysis results

3. Methods

3.1 Cell Culture

1. Cells are maintained in 10-cm cell culture dishes in a humidified (85–95%) 37 °C incubator with a 5% CO_2 atmosphere. Pass cells when they reach approximately 70–80% confluency, every 2–3 days. (*see* Note 1)
2. To passage cells, aspirate culture media and wash twice gently with 1 mL D-PBS. Add 1 mL of Trypsin-EDTA to cells, gently rock culture dish to distribute the Trypsin-EDTA and incubate for 5 min at room temperature. Add fresh HEK293T DMEM and mechanically wash dish to remove remaining cells, break up and suspend cells (also neutralizes the Trypsin-EDTA). (*see* Notes 4, 5 and 6)
3. For CRISPR-Cas9 editing, pass HEK293FT cells into a 24-well plate. For imaging, pass cells at 1:100 into a 35-mm glass bottom dish. To maintain cells, pass cells at 1:10 into a 10-cm culture dish for continued maintenance.

3.2 PolyJet Transfection (see Note 1)

1. To transfect plasmids into HEK 3293T/FT, add an optimized mass of plasmid DNA to 50 μL of transfection DMEM in a 2 mL microcentrifuge tube per imaging dish/well (for 6-well plate). Prepare a second tube by adding 3 μL of PolyJet to 50 μL of transfection DMEM. Then, add the 50-μL PolyJet-DMEM solution dropwise to the 50-μL plasmid-DMEM solution and incubate for 15 min at room temperature. (*see* Note 7 and 8)
    a. For transfecting FluoSTEP-ICUE into HEK 293FT cells with GFP_{11}-POI, we typically use 500 ng of FluoSTEP-ICUE plasmid DNA.
    b. For transfecting CRISPR-Cas9 components, see Section 3.3.
2. Add the 100-μL transfection solution to each well/dish dropwise and gently rock the dish back and forth to distribute the solution evenly.
3. Incubate at 37 °C for 18–24 h. (*see* Note 9)

3.3 Attaching GFP_{11} to a POI via CRISPR-Cas9

1. Design, generate, and test the gRNAs to determine the best gRNA for the genomic target.
    a. Choose whether to target the N- or C-terminus of the POI
    b. Design at least 3 gRNAs for the target region of the gene of interest (GOI), which encodes the POI. PAM sequences should be located as close as possible to the target region but can be outside the coding region.
    c. Individually clone each gRNA into the px459 plasmid (Golden Gate cloning protocol for CRISPR/Cas9 plasmids is readily available).
2. Use PolyJet transfection to transfect each cloned gRNA plasmid into HEK 293T cells. After 24 h, select cells using 1 μg/mL Puro. Harvest the remaining cells and extract genomic DNA. Amplify the target genomic region using PCR. Gel purify the PCR products and send for Sanger sequencing (*see* Note 10). To estimate the gRNA efficiency, upload the Sanger sequencing chromatograms and the target region to the Tracking of Indels by Decomposition (TIDE) tool. Use the gRNA efficiency to select the final gRNA for performing CRISPR-Cas9 insertion.
3. Design the HDR template to include the following (Figure 2) (*see* Note 11):
    a. GFP_{11} sequence (RDHMVLHEYVNAAGIT), linker region (GGG), and POI coding sequence. Linker sequences of 3–6 amino acids in length have been tested and shown to work successfully. The amino acid sequences for GFP_{11} with linkers are as follows:

        Targeting N-terminus: RDHMVLHEYVNAAGITGGG

        Targeting C-terminus: GGGRDHMVLHEYVNAAGIT

b. Silent mutation of the PAM sequence for gRNAs (*see* Note 12).

c. If targeting the N-terminus of the POI, include a START codon at the 5' end, and if targeting the C-terminus of the POI, add a stop codon at the 3' end.

d. HDR arms that are of equal length.

4. Synthesize the ssDNA HDR template ultramer (IDT ultramers or in house).

5. Transfect 1 μg of the selected gRNA plasmid along with 20 pmol of the ssDNA HDR template ultramer into HEK 293FT cells in 24-well plates via PolyJet transfection (*see* Note 13). Leave one well untransfected as a negative control. The next day, pass cells from each well into separate 60-mm dishes.

6. One day after passaging, add 1 μg/mL Puro to each 60-mm dish (optimized for HEK 293 cells) (*see* Notes 14 and 15). When no viable cells remain in the non-transfected well (2–3 days), exchange the media for Puro free HEK 293T DMEM.

7. One day after removing Puro, passage and resuspend cells appropriately for either of the following selection strategies (Figure 2):

a. Selection Strategy 1: Resuspend cells in FACS buffer containing DAPI. Using FACS, sort for DAPI-negative cells with the expected size and plate single cells into a 96-well plate with FACS DMEM (*see* Note 16). Single-cell colonies should be confluent in ~3 weeks.

b. Selection Strategy 2: Resuspend cells in DMEM and seed at 1:10 in a 60-mm dish. For positive selection, transfect $GFP_{1–10}$ into the edited GFP_{11} HEK 293FT cells. After 24 h, passage and resuspend the cells in FACS buffer. Use FACS to select for GFP-positive cells. After two weeks, use FACS to select against stable incorporation of $GFP_{1–10}$. Plate single cells into a 96-well plate containing FACS DMEM. Single-cell colonies should be confluent in ~3 weeks

8. Passage the confluent single-cell colonies (keeping half for expansion in normal HEK 293T media). Then extract genomic DNA from the cells (DNeasy Blood & Tissue Kit, Qiagen), perform PCR with primers designed to amplify the target region of the GOI (Q5 High-Fidelity Kit, New England Biolabs) (*see* Note 17), purify the PCR products via gel extraction (PureLink Quick Gel Extraction, Invitrogen), clone into TOPO PCR vectors (*see* Note 18), and perform Sanger sequencing to confirm knock-in.

3.4 Measuring endogenous, spatiotemporal cAMP dynamics at a POI

1. Before imaging, remove DMEM, gently wash cells twice with 1 mL of HBSS*, and then add 2 mL of HBSS as the final working volume. (*see* Note 19 and 20)

2. Power-on the lamp, microscope, filter changer, camera, and computer. Apply a small drop of immersion oil directly onto the objective (i.e., 1 drop from attached applicator tip). Avoid touching the applicator directly to the objective. Secure the

imaging dish to the microscope stage (*see* Note 21). Raise the objective until the immersion oil comes fully into contact with the glass bottom and bring the cells into focus while viewing through the eyepiece.

3. Load the METAFLUOR 7.7 application. Program imaging channels to acquire GFP direct, RFP direct, and G-R FRET intensities (Section 2.3). (*see* Note 22)

4. Turn off room lights. Find a field of view that contains multiple healthy cells expressing both green and red fluorescence at the appropriate subcellular location, indicating that FluoSTEP-ICUE is successfully reconstituted and targeted to the POI, and focus the image (*see* Note 23).

5. Adjust exposure times to optimize signal-to-noise and minimize photobleaching. Set the acquisition cycle period (between 10 and 120 s). (*see* Note 24)

    a. We used an exposure time of 500 ms and an acquisition cycle period of 30 sec.

6. It is helpful to view live FRET ratio traces during the experiment. Enable this feature if it is available in your software. Draw ROIs around select cells and one background region (area without any cells). (*see* Note 25)

7. Acquire images for 5–10 min to establish the baseline FluoSTEP emission ratios.

8. Remove 200 μL of HBSS* from the imaging dish and mix with a 2 mL aliquot of 1000X concentrated stimulus or inhibitor (Section 2.1) in a 2 mL microcentrifuge tube. Carefully apply the HBSS*-stimulus/inhibitor solution to the side of the dish and gently pipette to mix. Acquire images for 10–20 min, or until the FRET ratio change reaches a plateau. Repeat if imaging more than one stimulus or inhibitor cycle. (*see* Note 26)

    a. We have used 50 μM Fsk to activate ACs, increasing cAMP production. We have also used 10 μM Iso to stimulate cAMP via a biologically relevant agonist. We have used 100 μM IBMX to inhibit the majority of PDEs. Specific PDE inhibitors can be used for relevant cell lines and POIs.

9. Acquire images for the remainder of the experimental time-course. (*see* Note 27)

10. Save the data. Clean and power-down microscope.

3.5 Analyzing FluoSTEP-ICUE FRET data

1. To analyze imaging data, open the time-lapse files in METAFLUOR 7.7 and draw ROIs around each individual cell (Figure 3). Also, draw an ROI in the background (area without any cells). (*see* Note 28 and 29)

2. If your software has the function, program and run equations to calculate the FluoSTEP-ICUE Emission Ratios, see Eq. 1. Export the data into an Excel (Microsoft) worksheet. If not, perform calculations in Excel after the raw intensities are exported.

$$\frac{\text{FluoSTEP - ICUE Emission Ratio}}{\text{GFP Emission Intensity} - \text{GFP Background Emission Intensity}} = \frac{\text{GFP Emission Intensity} - \text{GFP Background Emission Intensity}}{\text{G - R FRET Emission Intensity} - \text{G - R FRET Background Emission Intensity}} \quad (1)$$

3. Plot graphs from the calculated FRET Emission Ratios using Excel or GraphPad Prism (or comparable software), as seen in Figure 3.

4. Notes

1. Depending on the parameters of your experiments, different cell lines can be used. The completed DMEM, concentration of Trypsin in Trypsin-EDTA, CRISPR-Cas9 strategy, and transfection method and efficiency may require adjusting to accommodate other cell lines. Additionally, splitting times may vary, so it is important to verify doubling times for each cell line used. If transfection is not efficient enough in the alternate cell line, viral expression is an alternative option.
2. The complete DMEM should contain phenol red to allow easy identification of wells containing single-cell colonies as the media will change from pink to yellow.
3. METAFLUOR 7.7 software requires a PC running compatible Microsoft Windows software.
4. All cell passage and transfection should be completed in a certified Biosafety Cabinet. All solutions should be made under sterile conditions. All solutions should be prepared with 18.2 MΩ-cm resistivity water, unless otherwise noted. DMEM should be pre-warmed to 37 °C and Trypsin-EDTA should be pre-thawed before use.
5. Be sure the cells are fully detached before continuing. A microscope can be used to confirm cell detachment.
6. Gently pipet cells up and down to break up cell clumps, but be careful not to over-pipet and damage the cells
7. Flick to thaw/mix plasmids. Vigorous mixing can cause shearing of the plasmid.
8. Transfection conditions depend on the size of the dish. The transfection outlined is optimized for a single-well of a 6-well dish or a single 35-mm imaging dish.
9. Alternative transfection strategies may require different incubation times and temperatures. Some transfection strategies (e.g., lipofectamine) require a change of media after incubating for a few hours to prevent cell death from the transfection reagents.
10. If gel-purified PCR products create messy chromatograms, PCR products can be cloned into the TOPO vector and then re-sent for Sanger sequencing.
11. Both double- and single-stranded HDR templates work for CRISPR/Cas9-mediated genome editing, but the efficiency and cellular context should be

considered [42]. Although longer HDR arms enable higher specificity and efficiency, long HDR templates can be more expensive; therefore, the feasibility and price of the HDR template needs to be considered.

12. If a silent PAM mutation is not possible, change the next possible nucleotide within the gRNA targeting region without altering the amino acid sequence. If multiple gRNAs efficiently edit the genome, silent mutations for each gRNA can be implemented into the HDR template.

13. Transfection of multiple gRNAs into the same cell may increase the chances of successful knock-in.

14. To determine the Puro concentration needed for selection, choose the lowest concentration of Puro that achieves 99% cell death by day 3. The following concentrations are suggested to construct a Puro selection curve: 0, 0.5, 1, 2, 3, 4, 5, 6, 7, 8, 9, 10 μg/mL.

15. If Puro is introduced too soon, the cells may still be too stressed from passaging for effective selection, leading to false negatives. If the cells grow for more than 1 day, wild-type cells may overgrow the gene-edited cells, as gene-edited cells may grow slower.

16. DAPI is unable to enter cells if the cell membrane is intact; therefore, cells without DAPI staining have survived Puro selection.

17. Genomic PCR can be challenging and typically leads to multiple bands.

18. 18. Some cell lines (e.g., HEK 293) are aneuploid, which may make it difficult to discern if cells are homozygous or heterozygous. Sequencing multiple TOPO PCR vectors allows for a rough estimation of the percentage of gene loci with successful knock-in of GFP_{11}.

19. Imaging is typically performed at room temperature. However, if cells need to be imaged at 37 °C to enhance the FRET response, an optional Heatable Insert P for Scanning Stage and Mechanical Stage (Zeiss) is used. When using this setup, an aliquot of HBSS* should be preheated to 37 °C prior to imaging.

20. Wash cells (e.g., HEK 293T) very carefully as the shear stress from washing can detach them from the dish and wash them away.

21. Securing the dish to the stage minimizes slight movement of the dish that may occur while imaging.

22. The G-R FRET channel records sensitized RFP emission intensity upon GFP excitation, the GFP channel records direct GFP emission intensity upon GFP excitation, and the RFP channel records direct RFP emission intensity upon RFP excitation.

23. When selecting the field of view for the experiment, consider these key criteria. First, cell morphology should be verified before starting an experiment, as healthy cells are required for successful imaging experiments. For instance, when imaging HEK 293T cells, select cells that are spread out and lying flat rather

than balled-up and rounded, as the latter could indicate unhealthy cells. Second, the fluorescence intensity of FluoSTEP-ICUE should be closely monitored. Unfortunately, a recommended range cannot be given as the intensity values will vary between microscope setups. Cells with a moderate intensity level are typically used. Cells with very dim fluorescence intensities will have a low signal-to-noise ratio, rendering changes in FRET difficult to visualize.

24. This exposure time and acquisition interval are a good starting point for most experiments. The exposure time can be adjusted to optimize the brightness of the reporter, but a longer exposure time can lead to increased photobleaching. Acquisition intervals can be increased to decrease photobleaching.

25. The live FRET ratio traces allow real-time observation during experiments but should be further processed for data presentation.

26. Stimulus and inhibitor drugs depend on cell type and POI. Keep aliquots of stimulus and inhibitor drugs on ice until they are ready to be used.

27. The selected ROIs need to remain in the same cellular region throughout the time series and may be manually readjusted to accommodate moving cells. Alternatively, cell tracking software (e.g., Imaris Track) can be used to overcome this problem.

28. Alternative software (e.g., MATLAB) can be used to export intensity values from imaging data. If software does not include cell tracking, use in conjunction with cell tracking software to accommodate moving cells. (*see* Note 27)

29. Only the GFP and G-R FRET intensities will be used to calculate the FluoSTEP-ICUE Emission Ratios (Eq. 1). RFP intensities are obtained to ensure the RFP acceptor is working properly throughout the time series.

References

1. Caretta A, Mucignat-Caretta C (2011) Protein kinase a in cancer. Cancers (Basel) 3 (1):913–926. doi:10.3390/cancers3010913 [PubMed: 24212646]
2. Beristain AG, Molyneux SD, Joshi PA, Pomroy NC, Di Grappa MA, Chang MC, Kirschner LS, Privé GG, Pujana MA, Khokha R (2015) PKA signaling drives mammary tumorigenesis through Src. Oncogene 34 (9):1160–1173. doi:10.1038/onc.2014.41 [PubMed: 24662820]
3. Nadella KS, Kirschner LS (2005) Disruption of Protein Kinase A Regulation Causes Immortalization and Dysregulation of D-Type Cyclins. Cancer Res 65 (22):10307. doi:10.1158/0008-5472.CAN-05-3183 [PubMed: 16288019]
4. Palorini R, Votta G, Pirola Y, De Vitto H, De Palma S, Airoldi C, Vasso M, Ricciardiello F, Lombardi PP, Cirulli C, Rizzi R, Nicotra F, Hiller K, Gelfi C, Alberghina L, Chiaradonna F (2016) Protein Kinase A Activation Promotes Cancer Cell Resistance to Glucose Starvation and Anoikis. PLOS Genetics 12 (3):e1005931. doi:10.1371/journal.pgen.1005931 [PubMed: 26978032]
5. Cheadle C, Nesterova M, Watkins T, Barnes KC, Hall JC, Rosen A, Becker KG, Cho-Chung YS (2008) Regulatory subunits of PKA define an axis of cellular proliferation/differentiation in ovarian cancer cells. BMC Medical Genomics 1 (1):43. doi:10.1186/1755-8794-1-43 [PubMed: 18822129]
6. Zimmerman NP, Roy I, Hauser AD, Wilson JM, Williams CL, Dwinell MB (2015) Cyclic AMP regulates the migration and invasion potential of human pancreatic cancer cells. Molecular carcinogenesis 54 (3):203–215. doi:10.1002/mc.22091 [PubMed: 24115212]

7. Burdyga A, Conant A, Haynes L, Zhang J, Jalink K, Sutton R, Neoptolemos J, Costello E, Tepikin A (2013) cAMP inhibits migration, ruffling and paxillin accumulation in focal adhesions of pancreatic ductal adenocarcinoma cells: effects of PKA and EPAC. Biochimica et biophysica acta 1833 (12):2664–2672. doi:10.1016/j.bbamcr.2013.06.011 [PubMed: 23797058]
8. Andersen JL, Kornbluth S (2013) The tangled circuitry of metabolism and apoptosis. Molecular cell 49 (3):399–410. doi:10.1016/j.molcel.2012.12.026 [PubMed: 23395270]
9. Suen DF, Norris KL, Youle RJ (2008) Mitochondrial dynamics and apoptosis. Genes & development 22 (12):1577–1590. doi:10.1101/gad.1658508 [PubMed: 18559474]
10. Stork PJ, Schmitt JM (2002) Crosstalk between cAMP and MAP kinase signaling in the regulation of cell proliferation. Trends in cell biology 12 (6):258–266. doi:10.1016/s0962-8924(02)02294-8 [PubMed: 12074885]
11. Beavo JA, Brunton LL (2002) Cyclic nucleotide research -- still expanding after half a century. Nat Rev Mol Cell Biol 3 (9):710–718. doi:10.1038/nrm911 [PubMed: 12209131]
12. Hayes JS, Brunton LL, Mayer SE (1980) Selective activation of particulate cAMP-dependent protein kinase by isoproterenol and prostaglandin E1. The Journal of biological chemistry 255 (11):5113–5119 [PubMed: 6154700]
13. Brunton LL, Hayes JS, Mayer SE (1981) Functional compartmentation of cyclic AMP and protein kinase in heart. Advances in cyclic nucleotide research 14:391–397 [PubMed: 6269390]
14. Adams SR, Harootunian AT, Buechler YJ, Taylor SS, Tsien RY (1991) Fluorescence ratio imaging of cyclic AMP in single cells. Nature 349 (6311):694–697. doi:10.1038/349694a0 [PubMed: 1847505]
15. Zaccolo M, De Giorgi F, Cho CY, Feng L, Knapp T, Negulescu PA, Taylor SS, Tsien RY, Pozzan T (2000) A genetically encoded, fluorescent indicator for cyclic AMP in living cells. Nat Cell Biol 2 (1):25–29. doi:10.1038/71345 [PubMed: 10620803]
16. Mehta S, Zhang J (2011) Reporting from the field: genetically encoded fluorescent reporters uncover signaling dynamics in living biological systems. Annual review of biochemistry 80:375–401. doi:10.1146/annurev-biochem-060409-093259
17. Kim N, Shin S, Bae SW (2021) cAMP Biosensors Based on Genetically Encoded Fluorescent/Luminescent Proteins. Biosensors 11 (2). doi:10.3390/bios11020039
18. Greenwald EC, Mehta S, Zhang J (2018) Genetically Encoded Fluorescent Biosensors Illuminate the Spatiotemporal Regulation of Signaling Networks. Chemical Reviews 118 (24):11707–11794. doi:10.1021/acs.chemrev.8b00333 [PubMed: 30550275]
19. Nikolaev VO, Bünemann M, Hein L, Hannawacker A, Lohse MJ (2004) Novel single chain cAMP sensors for receptor-induced signal propagation. The Journal of biological chemistry 279 (36):37215–37218. doi:10.1074/jbc.C400302200 [PubMed: 15231839]
20. Zaccolo M, Pozzan T (2002) Discrete microdomains with high concentration of cAMP in stimulated rat neonatal cardiac myocytes. Science 295 (5560):1711–1715. doi:10.1126/science.1069982 [PubMed: 11872839]
21. Mongillo M, McSorley T, Evellin S, Sood A, Lissandron V, Terrin A, Huston E, Hannawacker A, Lohse MJ, Pozzan T, Houslay MD, Zaccolo M (2004) Fluorescence resonance energy transfer-based analysis of cAMP dynamics in live neonatal rat cardiac myocytes reveals distinct functions of compartmentalized phosphodiesterases. Circulation research 95 (1):67–75. doi:10.1161/01.Res.0000134629.84732.11 [PubMed: 15178638]
22. Ponsioen B, Zhao J, Riedl J, Zwartkruis F, van der Krogt G, Zaccolo M, Moolenaar WH, Bos JL, Jalink K (2004) Detecting cAMP-induced Epac activation by fluorescence resonance energy transfer: Epac as a novel cAMP indicator. EMBO reports 5 (12):1176–1180. doi:10.1038/sj.embor.7400290 [PubMed: 15550931]
23. DiPilato LM, Zhang J (2009) The role of membrane microdomains in shaping beta2-adrenergic receptor-mediated cAMP dynamics. Molecular bioSystems 5 (8):832–837. doi:10.1039/b823243a [PubMed: 19603118]
24. Violin JD, DiPilato LM, Yildirim N, Elston TC, Zhang J, Lefkowitz RJ (2008) beta2-adrenergic receptor signaling and desensitization elucidated by quantitative modeling of real time cAMP dynamics. The Journal of biological chemistry 283 (5):2949–2961. doi:10.1074/jbc.M707009200 [PubMed: 18045878]

25. DiPilato LM, Cheng X, Zhang J (2004) Fluorescent indicators of cAMP and Epac activation reveal differential dynamics of cAMP signaling within discrete subcellular compartments. Proc Natl Acad Sci U S A 101 (47):16513–16518. doi:10.1073/pnas.0405973101 [PubMed: 15545605]
26. Jiang LI, Collins J, Davis R, Lin KM, DeCamp D, Roach T, Hsueh R, Rebres RA, Ross EM, Taussig R, Fraser I, Sternweis PC (2007) Use of a cAMP BRET sensor to characterize a novel regulation of cAMP by the sphingosine 1-phosphate/G13 pathway. The Journal of biological chemistry 282 (14):10576–10584. doi:10.1074/jbc.M609695200 [PubMed: 17283075]
27. Allen MD, DiPilato LM, Rahdar M, Ren YR, Chong C, Liu JO, Zhang J (2006) Reading dynamic kinase activity in living cells for high-throughput screening. ACS chemical biology 1 (6):371–376. doi:10.1021/cb600202f [PubMed: 17163774]
28. Wachten S, Masada N, Ayling LJ, Ciruela A, Nikolaev VO, Lohse MJ, Cooper DM (2010) Distinct pools of cAMP centre on different isoforms of adenylyl cyclase in pituitary-derived GH3B6 cells. Journal of cell science 123 (Pt 1):95–106. doi:10.1242/jcs.058594 [PubMed: 20016070]
29. Mohamed TMA, Oceandy D, Zi M, Prehar S, Alatwi N, Wang Y, Shaheen MA, Abou-Leisa R, Schelcher C, Hegab Z, Baudoin F, Emerson M, Mamas M, Di Benedetto G, Zaccolo M, Lei M, Cartwright EJ, Neyses L (2011) Plasma membrane calcium pump (PMCA4)-neuronal nitric-oxide synthase complex regulates cardiac contractility through modulation of a compartmentalized cyclic nucleotide microdomain. The Journal of biological chemistry 286 (48):41520–41529. doi:10.1074/jbc.M111.290411 [PubMed: 21965681]
30. Nikolaev VO, Bünemann M, Schmitteckert E, Lohse MJ, Engelhardt S (2006) Cyclic AMP imaging in adult cardiac myocytes reveals far-reaching beta1-adrenergic but locally confined beta2-adrenergic receptor-mediated signaling. Circulation research 99 (10):1084–1091. doi:10.1161/01.RES.0000250046.69918.d5 [PubMed: 17038640]
31. Zhang JZ, Lu TW, Stolerman LM, Tenner B, Yang JR, Zhang JF, Falcke M, Rangamani P, Taylor SS, Mehta S, Zhang J (2020) Phase Separation of a PKA Regulatory Subunit Controls cAMP Compartmentation and Oncogenic Signaling. Cell 182 (6):1531–1544.e1515. doi:10.1016/j.cell.2020.07.043 [PubMed: 32846158]
32. Sekar RB, Periasamy A (2003) Fluorescence resonance energy transfer (FRET) microscopy imaging of live cell protein localizations. The Journal of cell biology 160 (5):629–633. doi:10.1083/jcb.200210140 [PubMed: 12615908]
33. Tenner B, Getz M, Ross B, Ohadi D, Bohrer CH, Greenwald E, Mehta S, Xiao J, Rangamani P, Zhang J (2020) Spatially compartmentalized phase regulation of a Ca(2+)-cAMP-PKA oscillatory circuit. eLife 9. doi:10.7554/eLife.55013
34. Chakir K, Depry C, Dimaano VL, Zhu WZ, Vanderheyden M, Bartunek J, Abraham TP, Tomaselli GF, Liu SB, Xiang YK, Zhang M, Takimoto E, Dulin N, Xiao RP, Zhang J, Kass DA (2011) Galphas-biased beta2-adrenergic receptor signaling from restoring synchronous contraction in the failing heart. Science translational medicine 3 (100):100ra188. doi:10.1126/scitranslmed.3001909
35. Agarwal SR, Miyashiro K, Latt H, Ostrom RS, Harvey RD (2017) Compartmentalized cAMP responses to prostaglandin EP(2) receptor activation in human airway smooth muscle cells. British journal of pharmacology 174 (16):2784–2796. doi:10.1111/bph.13904 [PubMed: 28603838]
36. Godbole A, Lyga S, Lohse MJ, Calebiro D (2017) Internalized TSH receptors en route to the TGN induce local G(s)-protein signaling and gene transcription. Nat Commun 8 (1):443. doi:10.1038/s41467-017-00357-2 [PubMed: 28874659]
37. Di Benedetto G, Zoccarato A, Lissandron V, Terrin A, Li X, Houslay MD, Baillie GS, Zaccolo M (2008) Protein kinase A type I and type II define distinct intracellular signaling compartments. Circulation research 103 (8):836–844. doi:10.1161/circresaha.108.174813 [PubMed: 18757829]
38. Surdo NC, Berrera M, Koschinski A, Brescia M, Machado MR, Carr C, Wright P, Gorelik J, Morotti S, Grandi E, Bers DM, Pantano S, Zaccolo M (2017) FRET biosensor uncovers cAMP nano-domains at β-adrenergic targets that dictate precise tuning of cardiac contractility. Nat Commun 8:15031. doi:10.1038/ncomms15031 [PubMed: 28425435]
39. Cabantous S, Terwilliger TC, Waldo GS (2005) Protein tagging and detection with engineered self-assembling fragments of green fluorescent protein. Nature biotechnology 23 (1):102–107. doi:10.1038/nbt1044

40. Kamiyama D, Sekine S, Barsi-Rhyne B, Hu J, Chen B, Gilbert LA, Ishikawa H, Leonetti MD, Marshall WF, Weissman JS, Huang B (2016) Versatile protein tagging in cells with split fluorescent protein. Nature communications 7:11046–11046. doi:10.1038/ncomms11046

41. Mali P, Yang L, Esvelt KM, Aach J, Guell M, DiCarlo JE, Norville JE, Church GM (2013) RNA-guided human genome engineering via Cas9. Science 339 (6121):823–826. doi:10.1126/science.1232033 [PubMed: 23287722]

42. Bai H, Liu L, An K, Lu X, Harrison M, Zhao Y, Yan R, Lu Z, Li S, Lin S, Liang F, Qin W (2020) CRISPR/Cas9-mediated precise genome modification by a long ssDNA template in zebrafish. BMC Genomics 21 (1):67. doi:10.1186/s12864-020-6493-4 [PubMed: 31964350]

43. Tenner B, Zhang JZ, Kwon Y, Pessino V, Feng S, Huang B, Mehta S, and Zhang J (2021) FluoSTEPS: Fluorescent biosensors for monitoring compartmentalized signaling within endogenous microdomains. Science Advances. In Press.

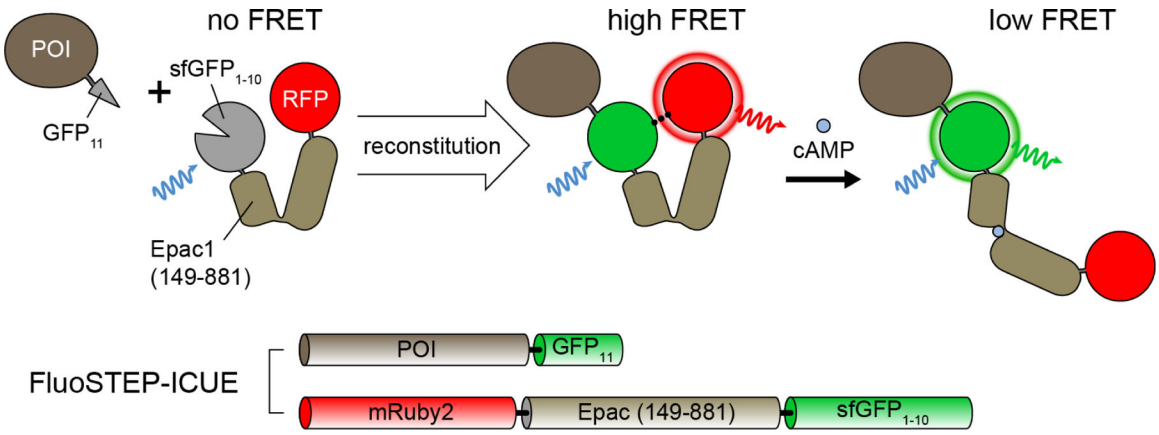

Figure 1: Design of FluoSTEP-ICUE.

(TOP) Schematic and (BOTTOM) domain structure of FluoSTEP-ICUE. The sensor consists of GFP11 fused to the N- or C-terminus of a POI at its endogenous genomic locus via CRISPR-Cas9 plus the Epac1(149–881)-based cAMP molecular switch sandwiched between mRuby2 and $sfGFP_{1–10}$. In cells co-expressing both sensor components, GFP11 and $sfGFP_{1–10}$ spontaneously reconstitute at the POI, yielding a functional, subcellularly targeted cAMP biosensor.

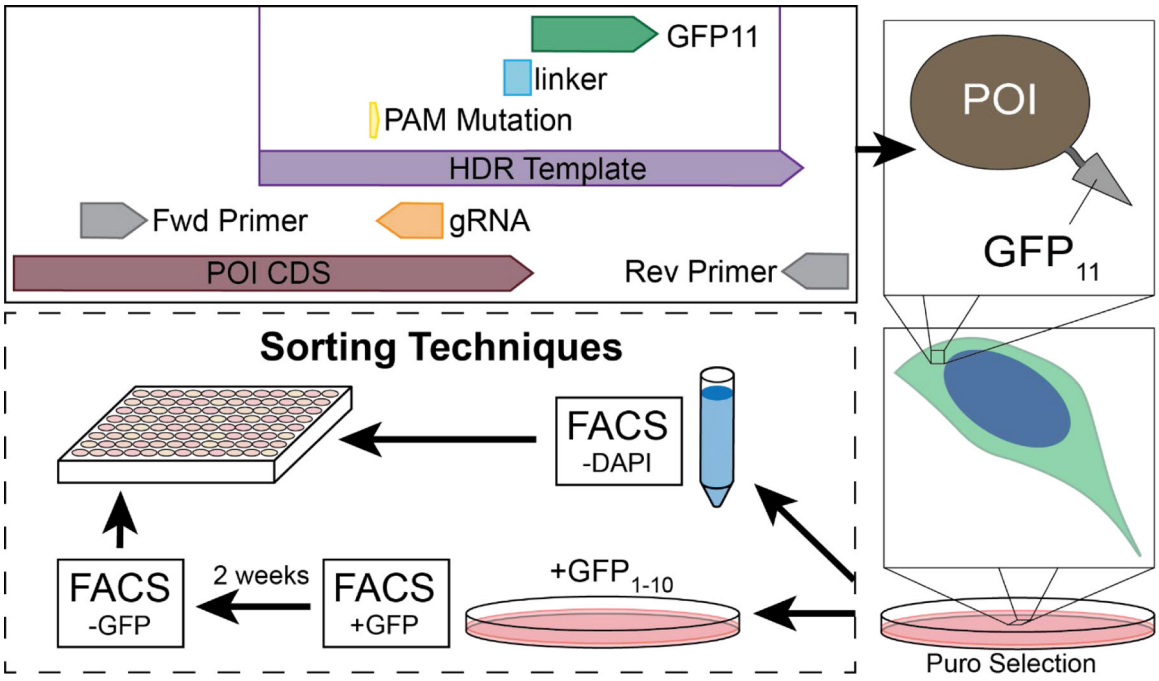

Figure 2: Cloning strategy to endogenously tag POI with GFP_{11}.

(TOP) Key components for the CRISPR-Cas9 strategy, including the HDR template, to insert GFP_{11} at the N- or C-terminus of the POI. (RIGHT) Once the POI is endogenously tagged with GFP_{11}, cells need to undergo Puro selection and FACS sorting to ensure the entire population of the cells have POI-GFP_{11}. (BOTTOM) Two FACS sorting techniques are outlined here. (1, top) Surviving cells are resuspended in FACS buffer containing DAPI. Use FACS to remove cells with DAPI expression, which indicates that the cell membrane is permeable and the cell did not survive Puro selection. (2, bottom) Surviving cells are passaged and transfected with $GFP_{1–10}$ to transiently complete the fluorescent protein. Use FACS to keep cells with GFP expression. Then, wait 2 weeks and repeat FACS to remove cells with GFP expression, indicating sustained integration of $GFP_{1–10}$ with POI-GFP_{11}.

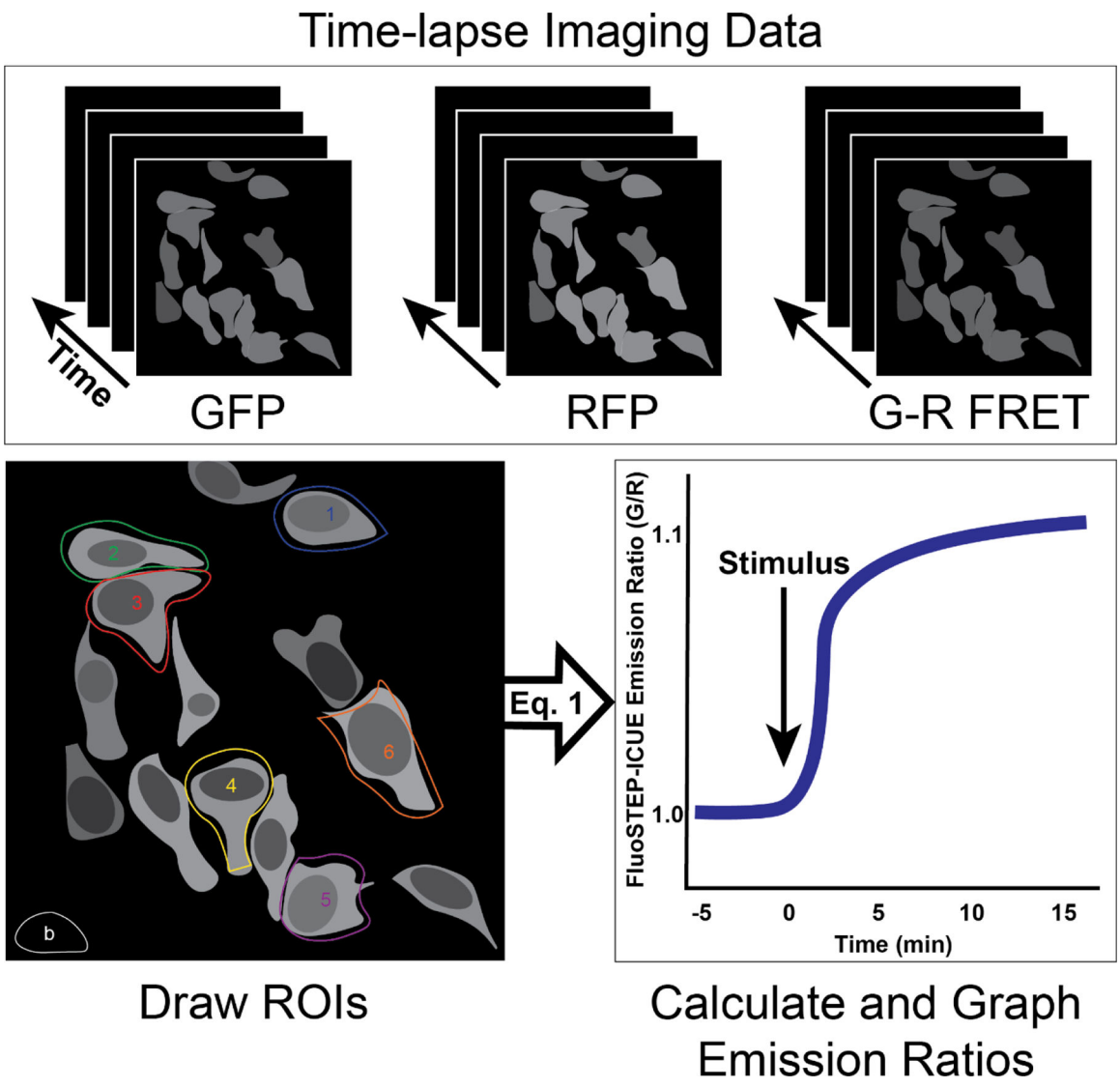

Figure 3: Processing and analyzing FluoSTEP-ICUE imaging data.

(TOP) Open GFP, RFP, and G-R FRET time-lapse imaging data in image analysis software. (BOTTOM, left) Create ROIs around healthy, attached cells expressing GFP, which indicates that the $GFP_{1–10}$ within FluoSTEP-ICUE incorporates with the GFP_{11} tagged to the POI. (BOTTOM, right) Use Equation 1 to calculate the FluoSTEP-ICUE emission ratios with the exported emission intensities from the GFP channel and G-R FRET channel. Graph the average FluoSTEP-ICUE emission ratios per time point.